Hindawi Publishing Corporation
International Journal of Photoenergy
Volume 2013, Article ID 929454, 9 pages
http://dx.doi.org/10.1155/2013/929454

Research Article

Preparation and Characterization of Cu_2ZnSnS_4 Thin Films and Solar Cells Fabricated from Quaternary Cu-Zn-Sn-S Target

Min Xie,[1] Daming Zhuang,[1] Ming Zhao,[1] Zuolong Zhuang,[2] Liangqi Ouyang,[1] Xiaolong Li,[1] and Jun Song[1]

[1] *Key Lab of Advanced Processing and Manufacturing, Ministry of Education, School of Material Science and Engineering, Tsinghua University, Haidian District, Beijing 100084, China*
[2] *Ningbo Nianxin Mechanic Company Limited, Zhejiang 315506, China*

Correspondence should be addressed to Daming Zhuang; dmzhuang@tsinghua.edu.cn

Received 16 September 2013; Revised 18 November 2013; Accepted 2 December 2013

Academic Editor: Raghu N. Bhattacharya

CZTS thin films were fabricated through sputtering from a quaternary Cu-Zn-Sn-S target, followed by a sulfurization process. CZTS thin-film solar cells were also fabricated and a highest efficiency of 4.04% was achieved. It has been found that obvious Zn loss occurs during the sputtering and poorly crystallized CZTS are formed in the sputtered films. The Zn loss leads to the appearance of SnS. A sulfurization process can obviously improve the crystallinity of CZTS and films with grain size of several hundred nanometers can be obtained after sulfurization. The optical band gap of the films is estimated to be 1.57 eV. The electrical properties of the 4.04% efficient solar cell were investigated and it has been found that cell has obvious deficiency in minority carrier lifetime. This deficiency should be responsible for the low J_{sc} and low V_{oc} of our cell.

1. Introduction

Thin-film solar cells based on the inorganic semiconductor CIGSe have demonstrated brilliant photovoltaic properties and great efforts have been devoted to the research of CIGSe thin film solar cells in recent years. A record efficiency of 20.3% has been achieved for CIGSe-based solar cells [1]. However, the wide application of CIGSe solar cells seems to be hindered by the shortage of In and Ga. Against this background, quaternary compound Cu_2ZnSnS_4 (CZTS) has attracted considerable attention as a promising candidate since it is totally composed of earth-abundant elements. CZTS has a crystal structure very similar to CIGS and also demonstrates good photovoltaic properties. It has a high absorption coefficient in the order of 10^4 cm^{-1} and a direct band gap of around 1.5 eV [2–4], close to the optimal band gap for single-junction solar cells. The theoretical limit conversion efficiency of CZTS thin-film solar cells reaches 32.2% [5].

Great efforts have been devoted to the fabrication of CZTS thin-film solar cells and various approaches have been developed, such as solution-based chemical synthesis methods [6–8], electroplating [9–11], sol-gel [12, 13], pulsed laser deposition [14, 15], evaporation [16, 17], and sputtering [18–20]. Since S and Se are in the same main group, $Cu_2ZnSn(S,Se)_4$ (CZTSS) is also classified as the CZTS family most of the time, although CZTSS and CZTS have different band gaps. A record efficiency of 11.1% has been achieved for CZTSS-based thin-film solar cells, through a solution-based chemical synthesis method [21]. The highest efficiency for pure CZTS-based thin-film solar cells reaches 8.4%, using an evaporation-based fabricating method [22].

Taking the future industrial production into account, sputtering is considered a more promising method for CZTS preparation, since sputtering has obvious advantages in achieving uniform deposition on large areas, which is very important for industrial production of thin-film solar

cells. For the sputtering methods, a typical process is a two-stage process, in which either metallic or S-containing precursors are firstly prepared through sputtering and then a sulfurization process is subsequently applied. Then, there can be three different categories, according to the type of targets used for precursor preparation. The first and most widely used category is sputtering from metallic targets, where metal or alloy targets are sputtered and metallic precursors are obtained [23, 24]. The second type is sputtering from S-containing targets, where binary ZnS, SnS, or Cu_2S targets are used for precursor preparation [25]. The third category is direct sputtering from quaternary Cu-Zn-Sn-S targets [26]. Compared to the former two catalogs, better uniformity and much smoother surface can be expected using the third category for CZTS preparation. However, research work about fabricating CZTS films using quaternary targets is rare so far. A highest efficiency of 6.48% was achieved by Katagiri and Jimbo through rf magnetron sputtering from CZTS compound targets [27]. Seol et al. successfully fabricated CZTS films through rf magnetron sputtering from a ceramic CZTS target in 2003 [28]. Inamdar et al. fabricated CZTS films with band gap of 1.55 eV through rf magnetron sputtering from a CZTS target in 2012 [29]. He et al. investigated the effect of postsulfurization on the properties of CZTS films deposited by rf sputtering from a quaternary target in 2013 [30]. Generally, it can be found that in all of those reported works rf magnetron sputtering was frequently used for the sputtering, which might not be favored in industrial production since rf sputtering devices are expensive and radiative. In this paper, on the one hand, CZTS thin films were prepared from a quaternary Cu-Zn-Sn-S target through middle-frequency magnetron sputtering with a frequency of 40 kHz, instead of rf magnetron sputtering. On the other hand, CZTS thin-film solar cells were also fabricated. The details of the preparation and characterization results of the CZTS thin films as well as solar cells were reported.

2. Experimental

Quaternary Cu-Zn-Sn-S target with atomic ratios of Cu : Zn : Sn : S = 1.8 : 1.1 : 0.9 : 3.0 was fabricated through hot pressed sintering. Cu_2S, ZnS, and SnS_2 powders were used. The purity of the target is higher than 99.99% and the size is 360 mm × 80 mm × 5 mm. The sputtering was carried out at room temperature using Ar as the working gas with a pressure of 0.7 Pa. The base pressure of the sputtering chamber is 3.0×10^{-3} Pa and the substrate to target distance is 50 mm. Both glass and Mo-coated glass were utilized as the substrate. The sputtering power for the quaternary target is 250 W and the sputtering time is 2 h.

The as-deposited precursors were then sent to a quartz tube sulfurizing system for sulfurization. The tube was evacuated to a base pressure of 2.0×10^{-3} Pa and then mixed gas of N_2 (60%, volume concentration) and H_2S (40%, volume concentration) was filled into the tube until the pressure reached 0.05 MPa. Samples in the tube were heated to 550°C at a heating rate of 20°C/min and kept at this temperature for 10 min. Finally the samples were cooled down to room temperature naturally.

Based on the obtained CZTS films, solar cells with a structure of Mo/CZTS/CdS/i-ZnO/AZO/Ni-Al grids were fabricated. Mo layer of about 1 μm thick was prepared by dc sputtering. CdS layer of around 80 nm thick was prepared by chemical bath deposition. I-ZnO and AZO layers were deposited by middle-frequency magnetron sputtering. Ni-Al grids of around 200 nm thick were prepared by evaporation.

The microstructures of the films were examined by X-ray diffraction (XRD, DMAX 2500 V) using Cu K_α irradiation (λ = 0.15418 nm), with an accelerating voltage of 40 kV. Raman scattering spectroscopy (Raman, RM 2000) was also used for microstructure analysis. The Raman detection was carried out at room temperature using 514.5 nm wavelength lasers as excitation source. The valence states of constituent elements of the films were characterized by X-ray photoelectron spectroscopy (XPS, 250 XI) with a monochromatic Al Kα (1486.6 eV) radiation source. The carbon 1s line corresponding to 285 eV was used for calibration of the binding energy. The surface and cross-section morphologies of the films were characterized by field emission scanning electron microscopy (FE-SEM, LEO-1530) at an accelerating voltage of 10 KV. The compositions of the films were analyzed by Inductively Coupled Plasma-Mass Spectrometry (ICP-MS, VISTA-MPX). The reflectance and transmittance spectra of the films were recorded by an UV-VIS-NIR spectrophotometer. The current-voltage characteristics of the solar cells were measured by a current-voltage testing device (Keithley 2000) using a solar simulator under AM 1.5 (100 mW/cm^2) illumination at room temperature. The quantum efficiency of the cells was recorded by a QT500 AD quantum efficiency testing system (crowtech Corp.) with a xenon light source and a monochromator with chopper frequency of 120 Hz. The time-resolved photoluminescence (TR-PL) measurement was performed on a finished cell using an Edinburg time-correlated single-photo counting system (F900), utilizing a 385 nm solid-state laser with a pulse width of around 3 ns and a repletion frequency of 40 kHZ as excitation source.

3. Results and Discussion

3.1. Structural Characterization. Figure 1 depicts the XRD and Raman patterns of the sputtered films and sulfurized films. For the sputtered films, except for Mo (110) peak, the broad peaks located at 28.5° and 47.3° indicate that CZTS with poor crystallinity might have formed (according to JCPDS 26-0575), as shown in Figure 1(a). Since the diffraction peaks of CZTS, Cu_2SnS_3, and ZnS phases are nearly the same, the actual phase corresponding to those two peaks cannot be identified as CZTS yet. Raman detection is needed for further confirmation. As shown in Figure 1(b), the only detected peak is the peak at 330 cm^{-1} for the sputtered films. This peak cannot be ascribed to either ZnS or Cu_2SnS_3 [31]. But the peak is also different from the typical main peak of CZTS, which often locates between 335 cm^{-1} and 338 cm^{-1} [32–34]. Peak at 330 cm^{-1} was rarely reported in research work about CZTS.

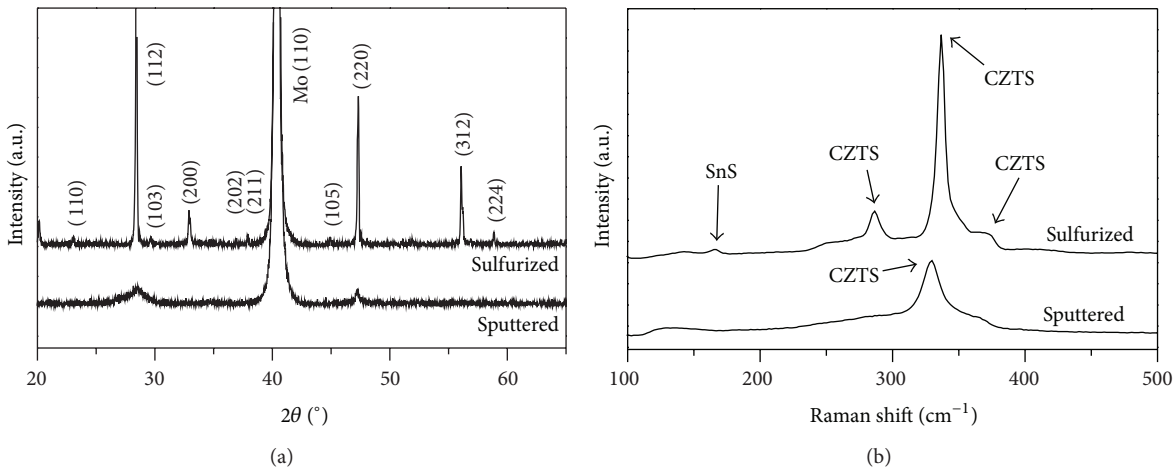

Figure 1: (a) XRD patterns of the sputtered and sulfurized films; (b) Raman patterns of the sputtered films and sulfurized films.

Only Khare et al. mentioned that the Raman peak of the A_1 mode of primitive mixed Cu-Au (PCMA) structure CZTS locates at 299.25 cm^{-1} [35]. Among the three different CZTS structures (kesterite structure (KS), stannite structure (SS), and primitive mixed Cu-Au structure (PCMA)), the most reported one is kesterite structure (KS). The typical Raman peaks corresponding to KS CZTS usually appear between 335 cm^{-1} and 338 cm^{-1}. The PCMA structure is a metastable state in which the atoms are partially in order. Then, it might be speculated that the peak at 330 cm^{-1} should correspond to PCMA CZTS, since a disordered arrangement is very likely to exist for the room temperature sputtered films. For further identification, X-ray photoelectron spectroscopy was carried out to examine the valence states of Cu, Zn, Sn, and S in the sputtered films and the results are shown in Figure 2. Peaks corresponding to Cu 2p, Zn 2p, Sn 3d, and S 2p can be observed in Figure 2(a). In Figure 2(b), the binding energies corresponding to Cu $2p_{3/2}$ and Cu $2p_{1/2}$ are 932.2 eV and 952.1 eV, respectively, indicating that copper is in Cu^+ state [36]. In Figure 2(c), the binding energies corresponding to Zn $2p_{3/2}$ and Zn $2p_{1/2}$ are 1021.5 eV and 1044.4 eV, respectively, revealing that zinc is in Zn^{2+} state [37]. In Figure 2(d), peaks corresponding to Sn $3d_{5/2}$ and Sn $3d_{3/2}$ are 486.4 eV and 494.8 eV, respectively, suggesting that tin is in Sn^{4+} state [38]. In Figure 2(e), the binding energies for S $2p_{3/2}$ and S $2p_{1/2}$ are 161.5 eV and 162.6 eV, respectively, revealing that sulfur is in sulfide state [39]. Consequently, it can be conducted that the above speculation is confirmed as true and the peak at 330 cm^{-1} in the Raman patterns should be ascribed to CZTS.

For the sulfurized films, except for Mo (110) peak, all of the rest diffraction peaks can be ascribed to CZTS, as denoted in Figure 1(a). Those peaks indicate that CZTS films with good crystallinity can be obtained after a sulfurization process. In Figure 1(b), peaks corresponding to kesterite CZTS appear at 286 cm^{-1}, 337 cm^{-1}, and 372 cm^{-1}, which are in good agreement with results reported elsewhere [40, 41]. However, a weak peak located at 160 cm^{-1} also appears in Figure 1(b), indicating that tiny amount of SnS exists [42]. Yet no peak corresponding to SnS phase appears in the corresponding XRD patterns. This result suggests that the amount of SnS is too small that it does not reach the detection limit of XRD measurement. In CZTS thin-film solar cells, the existence of SnS is often not favored, since SnS has high conductivity and a low band gap of around 1.1 eV. Yet the reason for its appearance will be discussed later.

Generally, it can be found that the sputtered films are mainly poorly crystallized CZTS and CZTS films with good crystallinity can be obtained after a sulfurization process. Yet tiny amount of SnS tends to exist in the films.

3.2. Compositional and Morphological Characterization. The chemical composition ratios of the quaternary target, the sputtered films and the sulfurized films, are shown in Table 1. It has been mentioned by many researchers that a chemical composition of Cu poor and slightly Zn rich is favorable for high-efficiency CZTS thin-film solar cells [43]. Naturally the target was initially designed as Cu rich and slight Zn rich here. However, the sputtered films were found to be Zn poor instead, as shown in Table 1. To clearly elucidate the content changes of Cu, Zn, and Sn elements after the sputtering and sulfurization processes, the relative concentrations of Cu, Zn, and Sn excluding S were also calculated and shown in Table 1. It can be seen that obvious Zn loss occurs during the sputtering. Such Zn loss should result from the evaporation of Zn during sputtering, since Zn has a rather high saturation pressure and a sublimation of Zn is likely to happen under frequent bombardment of Ar^+ toward the target. As a result, both the sputtered films, and sulfurized films become Zn poor. Such Zn shortage just results in Sn excess and consequently results in the appearance of SnS, as confirmed in above analysis. As for the sulfurization process, Table 1 reveals that the relative concentrations of Cu, Zn, and Sn excluding S are nearly the same as those in the sputtered films, indicating that element loss has not occured during sulfurization. Just as we expected, the S content in the films

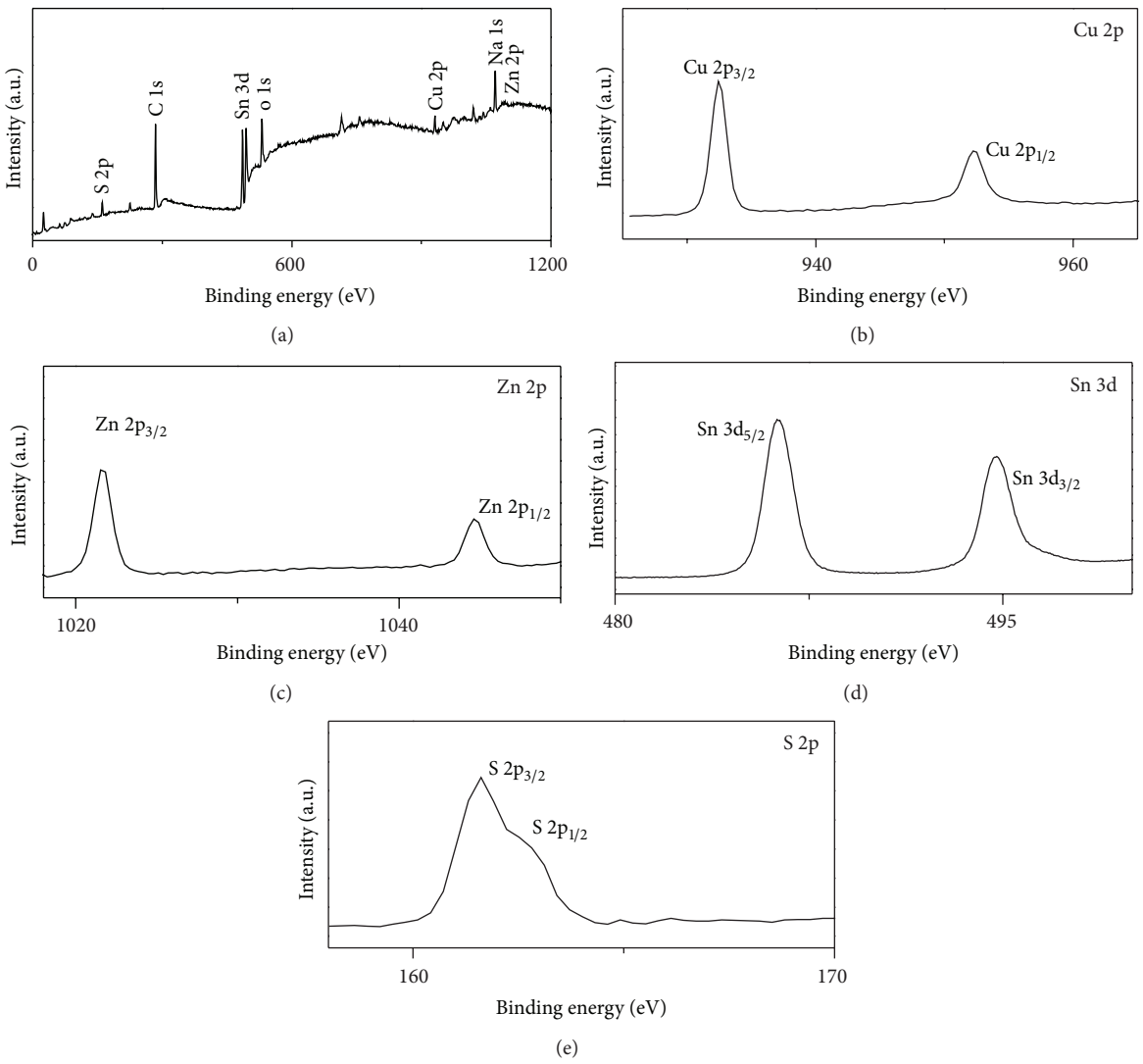

Figure 2: XPS spectra of sputtered films: (a) surveyscan; (b) core-level spectrum for Cu 2p; (c) core-level spectrum for Zn 2p; (d) core-level spectrum for Sn 3d; (e) core-level spectrum for S 2p.

Table 1: Composition ratios of the CZTS target, the sputtered films, and sulfurized films (atomic ratios).

	Cu/(Zn + Sn)	Zn/Sn	S/Metal	Cu/(Cu + Zn + Sn)	Zn/(Cu + Zn + Sn)	Sn/(Cu + Zn+ Sn)
The target	0.83	1.11	0.75	0.45	0.29	0.26
The sputtered films	0.92	0.87	0.75	0.48	0.24	0.28
The sulfurized films	0.92	0.83	0.97	0.48	0.24	0.28

increases after the sulfurization and a S/(Cu + Zn + Sn) ratio of approaching 1.0 can be achieved.

The surface and cross-section morphologies of the sputtered and sulfurized films were shown in Figure 3. In the sputtered films, the grain sizes are only several nanometers. Small grain size is often not favored in CZTS films since small grain sizes means that many grain boundaries exist and the recombination through grain boundaries can be severe. Yet, after the sulfurization process, the crystallinity can be obviously improved and CZTS grains with size of several hundred nanometers can be observed. The grains are densely packed and the surface is smooth. Such change once again suggests that a sulfurization process is quite necessary in the preparation of CZTS thin films, not only for the increase of S content, but also for the improvement of film crystallinity.

3.3. Optical Characterization. To evaluate the optical band gap of the sulfurized films, the reflection and transmittance spectra of the films were recorded by a UV-VIS-NIR spectrometer and the results are shown in Figure 4. Based on

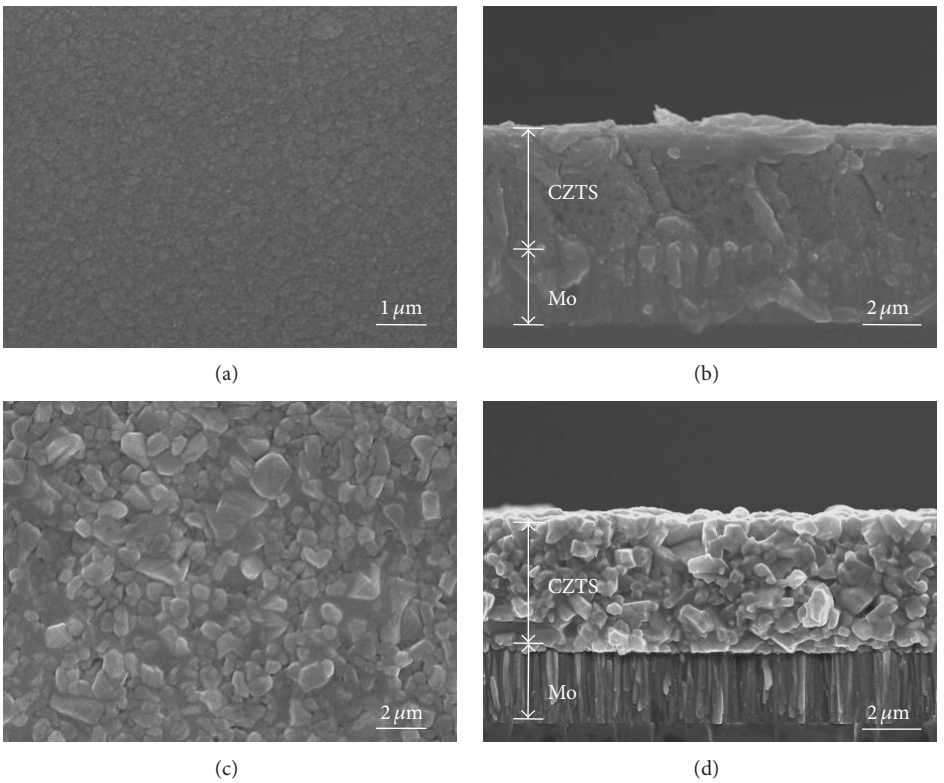

Figure 3: (a) Surface morphology of the sputtered films; (b) cross-section morphology of the sputtered films; (c) surface morphology of the sulfurized films; (d) cross-section morphology of the sulfurized films.

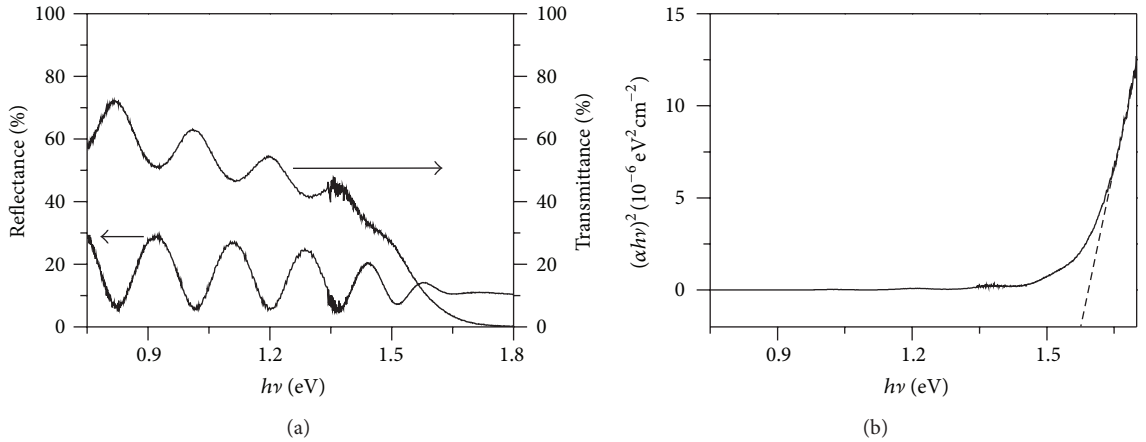

Figure 4: (a) Reflectance and transmittance spectra of CZTS films; (b) the $(\alpha h\nu)^2$ versus $h\nu$ plot of CZTS films.

the transmittance (T) and reflectance (R), the absorption coefficient (α) of the films can be obtained using the following equation [44]:

$$T = (1 - R)\, e^{-\alpha d}, \tag{1}$$

where R is the reflectance, T is the transmittance, and d is the thickness of the film. Based on the calculated α, the band gap of the films can be estimated using the following equation:

$$(\alpha h\nu)^n = A\left(h\nu - E_g\right), \tag{2}$$

where A is a constant and n is 2 for direct band gap materials and 1/2 for indirect band gap materials. Then, E_g can be determined by extrapolating the linear $(\alpha h\nu)^2$ versus $h\nu$ plots to $(\alpha h\nu)^2 = 0$. Accordingly, the band gap of the obtained CZTS films in this paper is estimated to be 1.57 eV, as depicted in Figure 4. This value is in good agreement with results reported elsewhere [44, 45].

3.4. Solar Cell Characterization. Based on the obtained CZTS thin films, CZTS thin-film solar cells with a structure of Mo/CZTS/CdS/i-ZnO/AZO/Ni-Al grids were fabricated.

Table 2: Solar cell efficiency results obtained in this paper.

Cell number	V_{oc}/mV	J_{sc}/(mA/cm^2)	FF/%	η/%	Area/cm^2
1	548.93	14.35	51.31	4.04	0.16
2	472.08	19.49	49.64	3.66	0.15
3	582.98	12.78	43.19	3.22	0.12
4	449.33	12.59	48.88	3.16	0.14
5	534.62	10.60	54.44	3.09	0.12
6	440.83	19.66	38.39	3.07	0.13

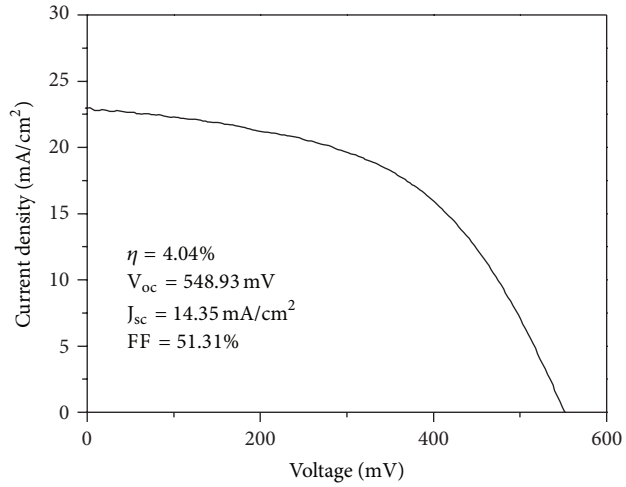

Figure 5: Current-voltage curve of the CZTS thin-film solar cells.

The efficiency results of obtained solar cells were depicted in Table 2. The different cell areas in Table 2 derive from manual scribing of the cells, instead of mechanical scribing. It can be seen that the achieved efficiencies are in the range of 3%-4% and the highest efficiency is 4.04%. Although the cells were prepared following the same process, the efficiencies were not totally the same. This should be related to the nonuniformity caused by the sulfurization process since an accurate control of the H_2S flow in the quartz tube is not achieved yet and the exact H_2S concentrations on top of each tiny area might not be totally the same. I-V curve of the 4.04% solar cell is shown in Figure 5. Yet, this efficiency is still lower than the highest efficiency of 8.4% for CZTS thin-film solar cells obtained by Shin et al.

For further comparison, the cell parameters of the 4.04% efficient solar cells obtained in this paper and the 8.4% efficient solar cells obtained by Shin et al. are listed in Table 3. It can be seen that our cell has obvious deficiencies in J_{sc} (~26% lower), followed by fill factor (~22% lower) and V_{oc} (~17% lower), where the numbers in parentheses indicate percentage shortage compared with the 8.4% efficient cells. The fill factor of a single-junction solar cell is often dependent on the diode quality factor A, the reverse saturation current J_0, the series resistance R_s, and parallel resistance R_p. The data in Table 3 reveals that the low fill factor of our cell should be derived from the high series resistance and low parallel resistance, since in most high-efficiency CZTS or CIGS solar cells a series resistance of less than 1 $\Omega\cdot$cm^2 and a parallel resistance of over 10^3 $\Omega\cdot$cm^2 are expected [46]. The causes for the high R_s and low R_p can vary. Bad electrode contacting or poor carrier transportation in the absorber layers can result in high R_s. The existence of pinholes or conductive phases can result in low R_p. In the above analysis, binary SnS is found to coexist in CZTS films. The existence of SnS is probably the main cause for the low R_p of our cells here, since SnS is a highly conductive phase. Except for FF, a lower V_{oc} is also observed for our cell. V_{oc} can be decided by the CZTS band gap, the J_{sc}, and J_0. In Table 3, the band gap of our CZTS films is higher than that of the 8.4% efficient solar cell, but the V_{oc} is still low. This is probably related to the low J_{sc}. As mentioned above, the J_{sc} of our cell is 26% lower than that of the 8.4% efficient cell. To clearly elucidate the cause for the lowered J_{sc}, the EQE (External Quantum Efficiency) curve of the 4.04% efficient solar cells was obtained and shown in Figure 6. The highest quantum efficiency is ~70% at wavelengths higher than 550 nm (the wavelength corresponding to the band gap of CdS) for our cell. But for the 8.4% efficient solar cells the corresponding efficiency is ~90%. This obvious difference naturally leads to the lowered J_{sc} and V_{oc} for our cell. Low quantum efficiency means that the quantity of collected photogenerated carriers is not kept at a high level. The recombination of holes and electrons in the films should often be responsible for low quantum efficiency. To check out whether severe recombination exists, the minority carrier lifetime of the solar cell was measured using TR-PL measurement device and the results are shown in Figure 7. The detection limit of the TR-PL device is 1 ns. As shown in the figure, a broad luminescent peak appears near 800 nm, corresponding to a band gap of around 1.5 eV, which agrees well with the optical measurement results. However, in the TR-PL spectra, the detected time-related luminescent spectra are almost the same as the background laser pulse spectra, which indicates that the minority carrier life time is too short that the detected curve almost overlaps with the excitation laser pulse curve. To get the exact value of minority carrier lifetime, fs laser-equipped TR-PL measurement device is needed. But unfortunately we have not found such device yet. But at least the results in Figure 7 suggest that the minority carrier life time of our solar cell should be less than 1 ns while for the 8.4% efficient cell it reaches 7.8 ns. Such a low minority carrier life time clearly reveals that severe recombination should exist in our cells and such recombination should be the main cause for the lowered quantum efficiency, as well as lowered J_{sc} and lowered V_{oc}. Yet the actual recombination mechanism that occurred in the films needs to be explored in future work.

4. Conclusion

CZTS thin films were fabricated through sputtering from a quaternary Cu-Zn-Sn-S target, followed by a sulfurization process. CZTS thin film solar cells were also fabricated and a highest conversion efficiency of 4.04% has been achieved. It has been found that obvious Zn loss occurs during the sputtering process and poorly crystallized CZTS are obtained after the sputtering. The Zn loss makes the film Zn poor and

Table 3: Parameters of the solar cell with 4.04% efficiency and with 8.04% efficiency.

η/%	V_{oc}/mV	J_{sc}/(mA/cm^2)	FF/%	A	R_s/Ω·cm^2	R_p/Ω·cm^2	J_0 (mA/cm^2)	CZTS band gap	CZTS grain size
4.04%	548.93	14.35	51.31	2.41	5.36	191.91	1.76e − 3	1.57	~200 nm
8.4%	661.00	19.50	65.80	2.00	3.66	—	1.40e − 3	1.45	~600 nm

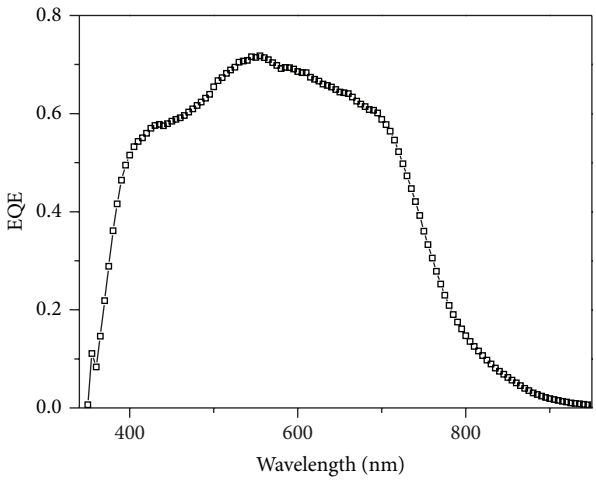

Figure 6: External quantum efficiency curves for the 4.04% efficient solar cell.

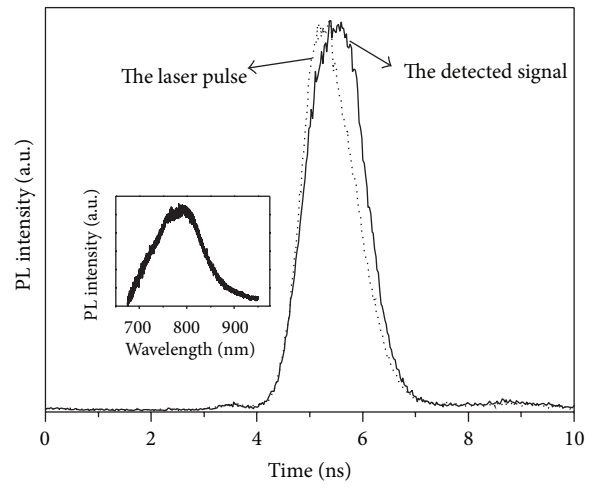

Figure 7: Time-resolved photoluminescence (TR-PL) spectrum of the cell at emission wavelength of 800 nm. The inset is the photoluminescence (PL) spectrum of the cell.

leads to the appearance of SnS. A sulfurization process can obviously improve the crystallinity of CZTS and increase the S content in the films. CZTS films with grain size of several hundred nanometers can be obtained after sulfurization. The optical band gap of the sulfurized films is estimated to be 1.57 eV. The electrical properties of the 4.04% efficient solar cell are investigated and a comparison between this cell and the cell with 8.4% efficiency is made. It has been found that our cell has obvious deficiency in minority carrier lifetime. This deficiency should be responsible for the low J_{sc} and low V_{oc} as well as a relatively low efficiency for our cell.

References

[1] P. Jackson, D. Hariskos, E. Lotter et al., "New world record efficiency for Cu(In,Ga)Se_2 thin-film solar cells beyond 20%," *Progress in Photovoltaics*, vol. 19, no. 7, pp. 894–897, 2011.

[2] K. Ito and T. Nakazawa, "Electrical and optical properties of stannite-type quaternary semiconductor thin films," *Japanese Journal of Applied Physics*, vol. 27, no. 11, pp. 2094–2097, 1988.

[3] H. Katagiri, N. Sasaguchi, S. Hando, S. Hoshino, J. Ohashi, and T. Yokota, "Preparation and evaluation of Cu_2ZnSnS_4 thin films by sulfurization of e-b evaporated precursors," *Solar Energy Materials and Solar Cells*, vol. 49, no. 1–4, pp. 407–414, 1997.

[4] N. Nakayama and K. Ito, "Sprayed films of stannite Cu_2ZnSnS_4," *Applied Surface Science*, vol. 92, pp. 171–175, 1996.

[5] W. Shockley and H. J. Queisser, "Detailed balance limit of efficiency of p-n junction solar cells," *Journal of Applied Physics*, vol. 32, no. 3, pp. 510–519, 1961.

[6] O. Zaberca, A. Gillorin, B. Durand, and J. Y. Chane-Ching, "A general route to the synthesis of surfactant-free, solvent-dispersible ternary and quaternary chalcogenide nanocrystals," *Journal of Materials Chemistry*, vol. 21, no. 18, pp. 6483–6486, 2011.

[7] N. M. Shinde, C. D. Lokhande, J. H. Kim, and J. H. Moon, "Low cost and large area novel chemical synthesis of Cu_2ZnSnS_4 (CZTS) thin films," *Journal of Photochemistry and Photobiology A*, vol. 235, pp. 14–20, 2012.

[8] T. Rath, W. Haas, A. Pein et al., "Synthesis and characterization of copper zinc tin chalcogenide nanoparticles: influence of reactants on the chemical composition," *Solar Energy Materials and Solar Cells*, vol. 101, pp. 87–94, 2012.

[9] C. P. Chan, H. Lam, and C. Surya, "Preparation of Cu_2ZnSnS_4 films by electrodeposition using ionic liquids," *Solar Energy Materials and Solar Cells*, vol. 94, no. 2, pp. 207–211, 2010.

[10] M. Jeon, Y. Tanaka, T. Shimizu, and S. Shingubara, "Formation and characterization of single-step electrodeposited Cu_2ZnSnS_4 thin films: effect of complexing agent volume," *Energy Procedia*, vol. 10, pp. 255–260, 2011.

[11] S. M. Pawar, B. S. Pawar, A. V. Moholkar et al., "Single step electrosynthesis of Cu_2ZnSnS_4 (CZTS) thin films for solar cell application," *Electrochimica Acta*, vol. 55, no. 12, pp. 4057–4061, 2010.

[12] K. Tanaka, N. Moritake, and H. Uchiki, "Preparation of Cu_2ZnSnS_4 thin films by sulfurizing sol-gel deposited precursors," *Solar Energy Materials and Solar Cells*, vol. 91, no. 13, pp. 1199–1201, 2007.

[13] M. Y. Yeh, C. C. Lee, and D. S. Wuu, "Influences of synthesizing temperatures on the properties of Cu_2ZnSnS_4 prepared by sol-gel spin-coated deposition," *Journal of Sol-Gel Science and Technology*, vol. 52, no. 1, pp. 65–68, 2009.

[14] S. M. Pawar, A. V. Moholkar, I. K. Kim et al., "Effect of laser incident energy on the structural, morphological and optical properties of Cu_2ZnSnS_4 (CZTS) thin films," *Current Applied Physics*, vol. 10, no. 2, pp. 565–569, 2010.

[15] L. Sun, J. He, H. Kong, F. Y. Yue, P. X. Yang, and J. H. Chu, "Structure, composition and optical properties of Cu_2ZnSnS_4 thin films deposited by Pulsed Laser Deposition method," *Solar Energy Materials and Solar Cells*, vol. 95, no. 10, pp. 2907–2913, 2011.

[16] T. Tanaka, D. Kawasaki, M. Nishio, Q. Guo, and H. Ogawa, "Fabrication of Cu_2ZnSnS_4 thin films by co-evaporation," *Physica Status Solidi C*, vol. 3, no. 8, pp. 2844–2847, 2006.

[17] I. Repins, C. Beall, N. Vora et al., "Co-evaporated $Cu_2ZnSnSe_4$ films and devices," *Solar Energy Materials and Solar Cells*, vol. 101, pp. 154–159, 2012.

[18] F. Y. Liu, Y. Li, K. Zhang et al., "In situ growth of Cu_2ZnSnS_4 thin films by reactive magnetron co-sputtering," *Solar Energy Materials and Solar Cells*, vol. 94, no. 12, pp. 2431–2434, 2010.

[19] K. Jimbo, R. Kimura, T. Kamimura et al., "Cu_2ZnSnS_4-type thin film solar cells using abundant materials," *Thin Solid Films*, vol. 515, no. 15, pp. 5997–5999, 2007.

[20] H. Araki, A. Mikaduki, Y. Kubo et al., "Preparation of Cu_2ZnSnS_4 thin films by sulfurization of stacked metallic layers," *Thin Solid Films*, vol. 517, no. 4, pp. 1457–1460, 2008.

[21] T. K. Todorov, J. Tang, S. Bag et al., "Beyond 11% efficiency: characteristics of state-of-the-art $Cu_2ZnSn(S,Se)_4$ solar cells," *Advanced Energy Materials*, vol. 1, no. 3, pp. 34–38, 2013.

[22] B. Shin, O. Gunawan, Y. Zhu, N. A. Bojarczuk, S. J. Chey, and S. Guha, "Thin film solar cell with 8.4% power conversion efficiency using an earth-abundant Cu_2ZnSnS_4 absorber," *Progress in Photovoltaics*, vol. 21, no. 1, pp. 72–76, 2011.

[23] P. A. Fernandes, P. M. P. Salomé, A. F. da Cunha, and B.-A. Schubert, "Cu_2ZnSnS_4 solar cells prepared with sulphurized dc-sputtered stacked metallic precursors," *Thin Solid Films*, vol. 519, no. 21, pp. 7382–7385, 2011.

[24] H. Yoo and J. Kim, "Growth of Cu_2ZnSnS_4 thin films using sulfurization of stacked metallic films," *Thin Solid Films*, vol. 518, no. 22, pp. 6567–6572, 2010.

[25] W. M. Oo, J. L. Johnson, A. Bhatia, E. A. Lund, M. M. Nowell, and M. A. Scarpulla, "Grain size and texture of Cu_2ZnSnS_4 thin films synthesized by cosputtering binary sulfides and annealing: effects of processing conditions and sodium," *Journal of Electronic Materials*, vol. 40, no. 11, pp. 2214–2221, 2011.

[26] J. Wang, S. Li, J. Cai, B. Shen, Y. Ren, and G. Qin, "Cu_2ZnSnS_4 thin films: facile and cost-effective preparation by rf-magnetron sputtering and texture control," *Journal of Alloys and Compounds*, vol. 552, pp. 418–422, 2013.

[27] H. Katagiri and K. Jimbo, "Development of rare metal-free CZTS-based thin film solar cells," in *Proceedings of the 37th IEEE Photovoltaic Specialists Conference (PVSC '11)*, pp. 3516–3521, 2011.

[28] J.-S. Seol, S.-Y. Lee, J.-C. Lee, H.-D. Nam, and K.-H. Kim, "Electrical and optical properties of Cu_2ZnSnS_4 thin films prepared by rf magnetron sputtering process," *Solar Energy Materials and Solar Cells*, vol. 75, no. 1-2, pp. 155–162, 2003.

[29] A. I. Inamdar Jeon K, H. Woo, W. Jung, H. Im, and H. Kim, "Controlled growth of Cu_2ZnSnS_4 (CZTS) thin films for heterojunction solar-cell applications," *Journal of the Korean Physical Society*, vol. 60, no. 10, pp. 1730–1734, 2012.

[30] J. He, L. Sun, K. Zhang et al., "Effect of post-sulfurization on the composition, structure and optical properties of Cu_2ZnSnS_4 thin films deposited by sputtering from a single quaternary target," *Applied Surface Science*, vol. 264, pp. 133–138, 2013.

[31] H. Katagiri, N. Ishigaki, T. Ishida, and K. Saito, "Characterization of Cu_2ZnSnS_4 thin films prepared by vapor phase sulfurization," *Japanese Journal of Applied Physics I*, vol. 40, no. 2, pp. 500–504, 2001.

[32] P. A. Fernandes, P. M. P. Salomé, and A. F. da Cunha, "Growth and Raman scattering characterization of Cu_2ZnSnS_4 thin films," *Thin Solid Films*, vol. 517, no. 7, pp. 2519–2523, 2009.

[33] P. A. Fernandes, P. M. P. Salomé, and A. F. da Cunha, "Study of polycrystalline Cu_2ZnSnS_4 films by raman scattering," *Journal of Alloys and Compounds*, vol. 509, no. 28, pp. 7600–7606, 2011.

[34] L. Sun, J. He, Y. Chen, F. Yue, P. Yang, and J. Chu, "Comparative study on Cu_2ZnSnS_4 thin films deposited by sputteringand pulsed laser deposition from a single quaternary sulfide target," *Journal of Crystal Growth*, vol. 361, pp. 147–151, 2012.

[35] A. Khare, B. Himmetoglu, M. Johnson, D. J. Norris, M. Cococcioni, and E. S. Aydil, "Calculation of the lattice dynamics and Raman spectra of copper zinc tin chalcogenides and comparison to experiments," *Journal of Applied Physics*, vol. 111, no. 8, Article ID 083707, 2012.

[36] C. Chory, F. Zutz, F. Witt, H. Borchert, and J. Parisi, "Synthesis and characterization of Cu_2ZnSnS_4," *Physica Status Solidi C*, vol. 7, no. 6, pp. 1486–1488, 2010.

[37] F. Jiang, H. L. Shen, and W. Wang, "Optical and electrical properties of Cu_2ZnSnS_4 film prepared by sulfurization method," *Journal of Electronic Materials*, vol. 8, no. 41, pp. 2204–2209, 2012.

[38] A. V. Moholkar, S. S. Shinde, A. R. Babar et al., "Synthesis and characterization of Cu_2ZnSnS_4 thin films grown by PLD: solar cells," *Journal of Alloys and Compounds*, vol. 509, no. 27, pp. 7439–7446, 2011.

[39] X. Zhang, X. Shi, W. Ye, C. Ma, and C. Wang, "Electrochemical deposition of quaternary Cu_2ZnSnS_4 thin films as potential solar cell material," *Applied Physics A*, vol. 94, no. 2, pp. 381–386, 2009.

[40] A.-J. Cheng, M. Manno, A. Khare, C. Leighton, S. A. Campbell, and E. S. Aydil, "Imaging and phase identification of Cu_2ZnSnS_4 thin films using confocal Raman spectroscopy," *Journal of Vacuum Science and Technology A*, vol. 29, no. 5, Article ID 051203, 2011.

[41] H. Yoo and J. Kim, "Comparative study of Cu_2ZnSnS_4 film growth," *Solar Energy Materials and Solar Cells*, vol. 95, no. 1, pp. 239–244, 2011.

[42] X. Fontané, L. Calvo-Barrio, V. Izquierdo-Roca et al., "In-depth resolved raman scattering analysis for the identification of secondary phases: characterization of Cu_2ZnSnS_4 layers for solar cell applications," *Applied Physics Letters*, vol. 98, no. 18, Article ID 181905, 2011.

[43] H. Katagiri, K. Saitoh, T. Washio, H. Shinohara, T. Kurumadani, and S. Miyajima, "Development of thin film solar cell based on Cu_2ZnSnS_4 thin films," *Solar Energy Materials and Solar Cells*, vol. 65, no. 1, pp. 141–148, 2001.

[44] F. Liu, K. Zhang, Y. Lai, J. Li, Z. Zhang, and Y. Liu, "Growth and characterization of Cu_2ZnSnS_4 thin films by dc reactive magnetron sputtering for photovoltaic applications," *Electrochemical and Solid-State Letters*, vol. 13, no. 11, pp. H379–H381, 2010.

[45] F. Jiang, H. Shen, W. Wang, and L. Zhang, "Preparation and properties of Cu_2ZnSnS_4 absorber and Cu_2ZnSnS_4/amorphous

silicon thin-film solar cell," *Applied Physics Express*, vol. 4, no. 7, Article ID 074101, 3 pages, 2011.

[46] P. J. Dale, K. Hoenes, J. Scragg, and S. Siebentritt, "A review of the challenges facing kesterite based thin film solar cells," in *Proceedings of the 34th IEEE Photovoltaic Specialists Conference (PVSC '09)*, pp. 2080–2085, Philadelphia, Pa, USA, June 2009.